Supplement of Geosci. Model Dev., 11, 3883–3902, 2018
https://doi.org/10.5194/gmd-11-3883-2018-supplement

Geoscientific Model Development
Open Access
EGU

Supplement of

LCice 1.0 – a generalized Ice Sheet System Model coupler for LOVECLIM version 1.3: description, sensitivities, and validation with the Glacial Systems Model (GSM version D2017.aug17)

Taimaz Bahadory and Lev Tarasov

Correspondence to: Lev Tarasov (lev@mun.ca)

1 Runoff routing

LOVECLIM has 26 predefined water discharge zones globally (colored cells in Fig. 1 (only the NH)) abutting continental margins within which the runoff flux calculated by the land model is uniformly distributed. The coupler then receives the GSM discharge at either continental margins or the terrestrial GSM grid boundaries (black lines in Fig. 1).

In the case of the continental margin, all the GSM drainage in regions bounded by same-color brackets are directed into LOVECLIM drainage cells with the similar color as the brackets. For instance, the GSM drainage south of Alaska between the two purple brackets is dumped into the four LOVECLIM purple cells in the same region. The LOVECLIM drainage module uniformly redistributes this discharge across the drainage cells within a given region.

Over the terrestrial GSM grid boundaries, the GSM runoff between same-color brackets are redirected to LOVECLIM drainage cells based on PD drainage maps. The GSM drainage in these regions is added to the runoff calculated by LOVECLIM from regions not covered by GSM grids. For instance, southern Europe runoff between the olive-green brackets are redirected into the Mediterranean, in addition to the runoff calculated by LOVECLIM from southern Europe and northern Africa.

For the south-eastern Eurasian margin of the GSM grid, the GSM runoff is directed to the Pacific ocean for the following reason. Most of the drainage in this largely dry region is northward except for that of the Caspian Sea watershed. As this sea is absent in LOVECLIM and all its mass-loss is evaporative, prevailing westerly winds would dictate predominantly eastward transport of moisture.

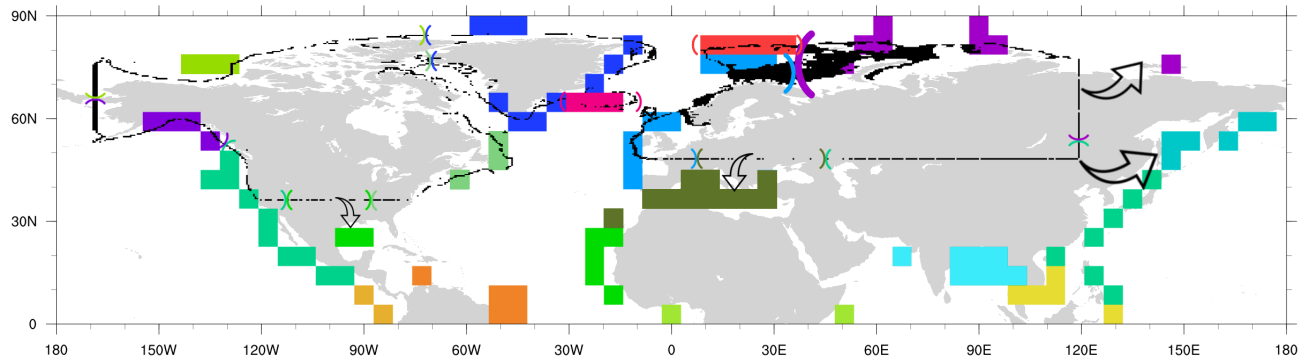

Figure 1. GSM (black lines) and LOVECLIM (colored cells) drainage sites. The colored brackets show the regions for which the GSM drainage is captured by the coupler and dumped into LOVECLIM drainage sites with the same color. The arrows show the GSM runoff at the GSM grid boundaries redirected to the appropriate ocean basin.

2 LOVECLIM 2-meter and surface temperature comparison

PDD ablation models are based on nominal 2 meter air temperatures and as such we use the 2 meter temperature from LOVECLIM. The use of surface temperatures in PDD models will give erroneous results as surface temperatures on ice and snow can not be above 0°C even when air temperature is. We note that the LOVECLIM based modelling of Roche et al. (2014) uses surface temperatures for PDD ablation calculation but without justification. To examine the implications of this choice, we compare LOVECLIM present-day bias and root mean square error (RMSE) to ERA reanalysis results (Uppala et al.) in Table 1. Given the simplified boundary layer physics of LOVECLIM, we also compare an average of LOVECLIM 2 meter and surface temperatures ($\bar{T}$). For surface massbalance contexts, summertime temperatures are most relevant. LOVECLIM July surface temperature (TS) has the worst RMSE relative to ERA40 globally and over both EA and NA. LOVECLIM 2 meter temperature ($T2m$) has the worst July RMSE over Antarctica and Greenland though the latter is only 0.5°C larger than that of

TS and $\bar{T}$. Furthermore, LOVECLIM *T2m* has the smallest July bias and RMSE for terrestrial NA and EA. LOVECLIM *T2m* also has the lowest global bias and RMSE for both July and February, over both land and ocean (except for being with 0.1°C of the lowest RSME for July global ocean). These results are for the default LOVECLIM tuning and retuning may provide better fits with $\bar{T}$.

Table 1. The difference between the LOVECLIM two meter air temperature (T2m), LOVECLIM surface temperature (TS), T2m and TS average ($\bar{T}$), and the ERA40 two meter air temperature (Uppala et al.), in Feburary and July at year 2000 A.D. The ERA40 temperature is corrected using the lapse-rate extracted from LOVECLIM to the same elevation as LOVECLIM topography. The means and root mean square errors (RMSE) are calculated by averaging the temperature differences over the each region (Global, North America (NA), Eurasia (EA), Greenland (Gr), and Antarctic), considering only the land mask (land), the ocean mask (ocean), and the boundaries shown in the map plots of the paper (all). Boldface values indicate the smallest mean differences (in magnitude) and RMSEs in each row.

			$T2m$		TS		$\bar{T}$	
			Mean	RMSE	Mean	RMSE	Mean	RMSE
Global	FEB	land	**1.003**	**4.531**	1.579	5.881	1.290	4.635
		all	**0.644**	**3.660**	1.951	4.467	1.297	3.727
		ocean	**0.504**	**3.261**	2.094	3.781	1.299	3.309
	JUL	land	**1.122**	**5.142**	4.359	6.984	2.74	5.162
		all	**0.522**	4.049	2.471	4.867	1.496	**3.972**
		ocean	**0.290**	3.537	1.740	3.738	1.015	**3.402**
NA	FEB	land	3.494	6.081	**0.549**	**3.353**	2.022	4.434
		all	4.069	6.399	**2.290**	**5.521**	3.179	5.607
		ocean	**5.008**	**6.889**	5.138	7.872	5.073	7.122
	JUL	land	**2.948**	**5.066**	5.952	7.190	4.450	5.833
		all	**2.587**	**4.964**	3.958	6.062	3.273	5.157
		ocean	1.997	4.793	**0.6951**	**3.507**	1.346	3.798
EA	FEB	land	1.542	**4.650**	-3.060	6.574	**-0.759**	5.018
		all	**-0.201**	5.477	-2.764	6.626	-1.482	**5.449**
		ocean	-4.542	7.131	**-2.026**	6.753	-3.284	**6.398**
	JUL	land	**3.209**	**4.113**	8.284	9.323	5.746	6.597
		all	**2.181**	**3.821**	5.830	8.139	4.005	5.835
		ocean	-0.3784	**2.974**	**-0.278**	3.842	-0.328	3.232
GR	FEB	land	3.107	7.846	**-0.281**	8.140	1.413	**7.394**
		all	**2.979**	**7.471**	3.753	9.349	3.366	7.952
		ocean	**2.895**	**7.215**	6.400	10.060	4.648	8.299
	JUL	land	3.012	3.945	**1.192**	3.477	2.102	**3.455**
		all	3.027	4.042	**1.545**	**3.452**	2.286	3.489
		ocean	3.036	4.104	**1.777**	**3.435**	2.406	3.510
AA	FEB	land	3.499	7.151	**-0.771**	**5.361**	1.364	5.726
		all	1.630	5.139	**0.668**	**4.521**	1.149	4.546
		ocean	**0.722**	**3.796**	1.366	4.051	1.044	3.845
	JUL	land	6.983	13.250	-5.872	10.310	**0.556**	**9.760**
		all	**-0.198**	10.170	-4.292	9.333	-2.245	**8.797**
		ocean	-3.683	**8.276**	**-3.525**	8.818	-3.604	8.290

References

Roche, D. M., Dumas, C., Bügelmayer, M., Charbit, S., and Ritz, C.: Adding a dynamical cryosphere to iLOVECLIM (version 1.0): coupling with the GRISLI ice-sheet model, Geoscientific Model Development, 7, 1377–1394, https://doi.org/10.5194/gmd-7-1377-2014, 2014.

Uppala, S. M., KÅllberg, P. W., Simmons, A. J., Andrae, U., Costa, B. V. D., Fiorino, M., Gibson, J. K., Haseler, J., A., H., Kelly, G. A., Li, X., Onogi, K., Saarinen, S., Sokka, N., Allan, R. P., Andersson, E., Arpe, K., Balmaseda, M. A., Beljaars, A. C. M., Berg, L. V. D., J., B., N., B., S., C., F., C., A., D., M., D., M., F., M., F., S., H., E., H., J., H. B., L., I., M., J. P. A. E., R., J., P., M. A., J.-F., M., J.-J., M., A., R. N., W., S. R., P., S., A., S., E., T. K., A., U., D., V., P., V., and J., W.: The ERA-40 re-analysis, Quarterly Journal of the Royal Meteorological Society, 131, 2961–3012, https://doi.org/10.1256/qj.04.176, https://rmets.onlinelibrary.wiley.com/doi/abs/10.1256/qj.04.176.